ISSN 1674-1056
http://cpb.iphy.ac.cn
http://iopscience.iop.org/cpb
中国物理 B
Chinese Physics
中国物理
Chinese Physics B

Broadband visible light absorber based on ultrathin semiconductor nanostructures

Lin-Jin Huang(黄林锦), Jia-Qi Li(李嘉麒), Man-Yi Lu(卢漫仪), Yan-Quan Chen(陈彦权), Hong-Ji Zhu(朱宏基), Hai-Ying Liu(刘海英)

Citation: Chin. Phys. B . 2020, 29(1): 014201 . **doi:** 10.1088/1674-1056/ab5787
Journal homepage: http://cpb.iphy.ac.cn; http://iopscience.iop.org/cpb

What follows is a list of articles you may be interested in

Comparison of three kinds of polarized Bessel vortex beams propagating through uniaxial anisotropic media

Jia-Wei Liu(刘佳伟), Hai-Ying Li(李海英), Wei Ding(丁炜), Lu Bai(白璐), Zhen-Sen Wu(吴振森), Zheng-Jun Li(李正军)
Chin. Phys. B . 2019, 28(9): 094214 . **doi:** 10.1088/1674-1056/ab37f5

Flexible broadband polarization converter based on metasurface at microwave band

Qi Wang(王奇), Xiangkun Kong(孔祥鲲), Xiangxi Yan(严祥熙), Yan Xu(徐岩), Shaobin Liu(刘少斌), Jinjun Mo(莫锦军), Xiaochun Liu(刘晓春)
Chin. Phys. B . 2019, 28(7): 074205 . **doi:** 10.1088/1674-1056/28/7/074205

Light propagation characteristics of turbulent plasma sheath surrounding the hypersonic aerocraft

Chunjing Lv(吕春静), Zhiwei Cui(崔志伟), Yiping Han(韩一平)
Chin. Phys. B . 2019, 28(7): 074203 . **doi:** 10.1088/1674-1056/28/7/074203

Loss induced negative refraction and super-prism effect at highly absorptive interface

Jian Wu(吴坚), Tao Wang(王涛), Tianyue Hou(侯天悦), Xuefen Kan(阚雪芬), Cheng Yin(殷澄), Pu Zhou(周朴), Zhuangqi Cao(曹庄琪)
Chin. Phys. B . 2019, 28(5): 054201 . **doi:** 10.1088/1674-1056/28/5/054201

Physics of quantum coherence in spin systems

Maimaitiyiming Tusun(麦麦提依明·吐孙), Xing Rong(荣星), Jiangfeng Du(杜江峰)
Chin. Phys. B . 2019, 28(2): 024204 . **doi:** 10.1088/1674-1056/28/2/024204

Broadband visible light absorber based on ultrathin semiconductor nanostructures*

Lin-Jin Huang(黄林锦), Jia-Qi Li(李嘉麒), Man-Yi Lu(卢漫仪), Yan-Quan Chen(陈彦权), Hong-Ji Zhu(朱宏基), and Hai-Ying Liu(刘海英)†

Guangdong Provincial Key Laboratory of Nanophotonic Functional Materials and Devices, School for Information and Optoelectronic Science and Engineering, South China Normal University, Guangzhou 510006, *China*

(Received 1 August 2019; revised manuscript received 5 September 2019; accepted manuscript online 14 November 2019)

It is desirable to have electromagnetic wave absorbers with ultrathin structural thickness and broader spectral absorption bandwidth with numerous applications in optoelectronics . In this paper, we theoretically propose and numerically demonstrate a novel ultrathin nanostructure absorber composed of semiconductor nanoring array and a uniform gold substrate. The results show that the absorption covers the entire visible light region, achieving an average absorption rate more than 90% in a wavelength range from 300 nm to 740 nm and a nearly perfect absorption from 450 nm to 500 nm, and the polarization insensitivity performance is particularly great. The absorption performance is mainly caused by the electrical resonance and magnetic resonance of semiconductor nanoring array as well as the field coupling effects. Our designed broadband visible light absorber has wide application prospects in the fields of thermal photovoltaics and photodetectors.

Keywords: ultrathin nanostructures, electrical resonance, magnetic resonance, polarization insensitivity

PACS: 42.25.Bs, 78.67.Pt, 78.20.Ci **DOI:** 10.1088/1674-1056/ab5787

1. Introduction

In the past decade, electromagnetic (EM) metamaterials have attracted extensive attention from both scientific and engineering communities due to their ability to achieve unique properties.[1,2] The peculiar performances of metamaterials have enabled many novel applications, such as invisibility cloaks,[3,4] perfect lenses,[5] metalenses,[6–8] perfect absorption,[9] *etc*. In particular, perfect absorbers made of metamaterial have been extensively studied due to broad application prospects since the Landy experiment in 2008.[10] The conventional perfect absorber is usually based on the three-layer structure of metal–dielectric–metal (MDM), for instance, Aydin *et al.* proposed a perfect absorber, and designed a thin dielectric spacer to accomplish the strong plasma coupling between the top resonator and the bottom metal film,[11] thus achieving perfect absorption. The traditional MDM absorber is widely used in a variety of designs.[11–17] However, the practical application of the absorber can be limited due to the inherent damping loss in the metal.[18,19]

To reduce the absorption loss, the researchers turned their attention to high refractive index dielectric materials. The resonant behavior of the incident light in high index dielectric nanoparticles can excite the mode similar to metal nanoparticles,[20] reproduce many subwavelength effects demonstrated in the plasma due to the localization of the electric field, but without great losses or energy dissipation into heat.[21] In addition, the dielectric metamaterial unit can support electrical and magnetic dipole response due to Mie resonance, and the coexistence of strong electromagnetic and multipole resonances, their interference and the resonance enhancement of magnetic fields in dielectric nanoparticles can produce rich applications.[22–25] More significantly, the electromagnetic oscillation of dielectric nanoparticles is positively correlated with the effective refractive index. So the semiconductor materials such as silicon (Si), germanium (Ge), and gallium arsenide (GaAs) are of great interest to many researchers due to high refractive index, and they have begun to study the semiconductor absorbers. Liu *et al.* proposed a semiconductor absorber with an aluminum (Al) ring intercalated with a silicon disc array[26] and obtained four narrow-band perfect absorption peaks by utilizing the plasmon resonance coupling of silicon and Al. The narrow-band perfect absorber is easily applied to sensing, but numerous optoelectronics applications always need the electromagnetic wave absorbers with ultrathin structural thickness and broader spectral absorption bandwidth.[27–32] So Liu *et al.* reported a broadband semiconductor absorber composed of a GaAs cylinder resonator and an ultrathin GaAs film on an Al substrate.[33] It possessed an absorption band with bandwidth up to 340 nm in the near-infrared region. However, most of the researches on semiconductor-based metamaterial absorbers were carried out at THz or infrared wavelengths, and the research results of visible light absorbers designed with semiconductor materials are still less so far. Zhu *et al.* also proposed an ultra-thin broadband visible light absorption absorber composed of silicon nanostructure,[34] a silicon dioxide (SiO_2) spacer layer and

*Project supported by the Natural Science Foundation of Guangdong Province, China (Grant Nos. 2018A030313854 and 2016A030313851).

†Corresponding author. E-mail: hyliu@scnu.edu.cn

© 2020 Chinese Physical Society and IOP Publishing Ltd

a gold substrate, but its absorption does not cover the entire visible light wave band. Thus, it can be seen that the design of broadband visible light absorbers based on semiconductor ultrathin nanostructures is still significant, and relevant research has great potential in the application of visible light.

In this paper, we design a broadband visible light absorber based on semiconductor ultrathin nanostructures. The broadband visible light absorber consists of a hexagonal lattice of GaAs nanoring array and a gold substrate. The ideal broadband absorption results from the electrical resonance and magnetic resonance of semiconductor nanoring array as well as the field coupling effects. The proposed absorber can achieve a bandwidth absorption of 440 nm (above 80%) in the visible region with an average absorption rate over 90%. This semiconductor-based metamaterial absorber is simple in structure and can achieve bandwidth absorption of visible light with high absorption performance only by using simple geometric array. The proposed GaAs nanoring absorber will have great potential in the field of solar energy, photodetectors, and thermal imaging.

2. Geometric parameters of the GaAs absorber

Figures 1(a) and 1(b) show the proposed broadband visible light absorber, which is made of a layer of GaAs nanoring array on a gold substrate, and the surrounding material is assumed to be air. The gold substrate at the bottom is 100-nm thick, making it impossible for incident light to pass through. The hexagonal GaAs nanoring array has a thickness (h) of 60 nm, an outer diameter (D) of 220 nm, an inner diameter (d) of 120 nm, and a period (P) of 300 nm. The fabrication process of proposed metamaterials is compatible with popular nanofabrication technologies, such as electron beam lithography.[35]

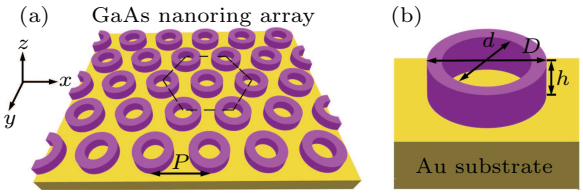


Fig. 1. (a) Schematic diagram of hexagonal "GaAs nanoring array" broadband visible light absorber. (b) Magnified one of its units. The absorber consisting of hexagonal GaAs nanoring array and a uniform gold substrate. The parameters are set to be $P = 300$ nm, $D = 220$ nm, $d = 120$ nm, and $h = 60$ nm.

We use the finite difference time domain (FDTD) to simulate the reflectivity, transmittance, absorption, and field distribution of the absorber.[36] The light source is a plane wave that is normally incident, and the complex refractive index of relevant materials is cited from data of Palik.[37] Periodic boundary conditions are used to present a periodic array in the x direction and also in the y direction, while a perfectly matched layer (PML) is applied along the z direction to eliminate boundary scattering. The reflectance spectrum (R) is recorded by a two-dimensional (2D) frequency domain power monitor that is perpendicular to the xoy plane.

3. Numerical analysis and discussion

3.1. Performances and principles

Figure 2 shows the optical spectra of the proposed broadband visible light absorber at normal incidence, involving reflection (R), absorption (A), and transmission (T). For light absorption A, it can be obtained from the equation: $A = 1 - R - T$, where R denotes reflection (R) and T represents transmission (T). The incident light will not pass through the substrate when the gold substrate is thicker than the penetration depth of the incident light, so the blue line which represents the transmitted light (T) is essentially zero, and absorption $A = 1 - R$. As can be seen from the red line in Fig. 2, the absorption of the proposed absorber covers the entire visible light region, which can achieve an absorption rate of above 80% covering the wave band from 300 nm to 740 nm. Moreover, the absorption rate is relatively flat and close to a prefect absorption rate in a wavelength range from 300 nm to 500 nm because of the excitation of the electrical resonance and magnetic resonance in the GaAs nanoring array. After that, the other two absorption peaks are caused by the field coupling between the structures. By theoretical calculations, the absorber can achieve an average absorption rate of more than 90% in the wavelength range from 300 nm to 740 nm.

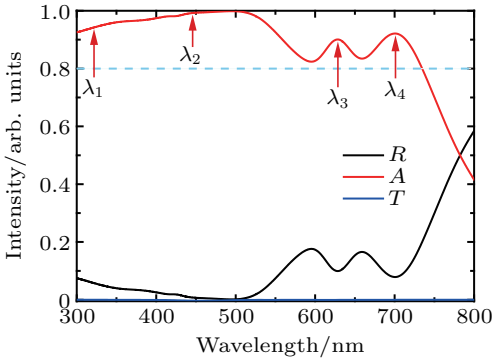


Fig. 2. Spectrum intensities of the GaAs absorber.

In order to fully characterize the physical mechanism of the absorption peak observed in the absorption spectrum, we further investigate the field distributions of the absorber in the xoy and xoz plane at different wavelengths ($\lambda_1 = 320$ nm, $\lambda_2 = 450$ nm, $\lambda_3 = 650$ nm, $\lambda_4 = 704$ nm) as shown in Fig. 3. The position at 55 nm above the substrate is selected to analyze the field distribution of its xoy plane. In the electric field distribution at $\lambda_1 = 320$ nm shown in Fig. 3(a), the strong electric field is concentrated in the inner and outer parts of the nanoring, which indicates that strong electric resonance is excited

in the GaAs nanoring array. It is also noticed that the electric field radiates outward from the top of the nanoring and is located in air above the nanoring, which indicates that the surface lattice resonance is generated when strong electric resonance is excited. Figure 3(b) shows the magnetic field distribution of resonance at $\lambda_2 = 450$ nm, and it can be observed that the strong magnetic field is located on both sides of the y direction of the GaAs nanoring, and there are also strong magnetic hot spots on both sides of the x direction of the GaAs nanoring. These characteristics indicate that the strong magnetic resonance is excited in the structure.[22] Meanwhile, the enhancement in magnetic field occurs not only in the ring, but also on the metal surface between the ring and the ring. The strong magnetic resonance of the ring itself and the interaction with the metal surface produce a perfect absorption of the incident light. Then we analyze the field distributions at the two peaks of the long wavelength. The electric field distribution at $\lambda_3 = 650$ nm shown in Fig. 3(c) indicates that the absorption peak is caused mainly by the strong coupling of the electric field. The overlap of the electric field interaction between the outer surface and the inner surface of the ring makes the coupling between the electric fields stronger. In addition, relatively strong electric field can also be found near the surface of the metal substrate. This phenomenon indicates that the propagating plasma resonance mode is also excited near the gold film. In Fig. 3(d), it is revealed that the magnetic field distribution of another absorption peak at $\lambda_4 = 704$ nm has relatively obvious characteristic. The magnetic field is distributed inside the ring, between adjacent rings, and on the metal surface, indicating that the absorption peak is the result of magnetic field coupling. The optical field distribution at these resonant wavelengths demonstrates that the electrical and magnetic resonance, as well as the field coupling effects present in the GaAs absorber together lead to broadband visible light absorption.

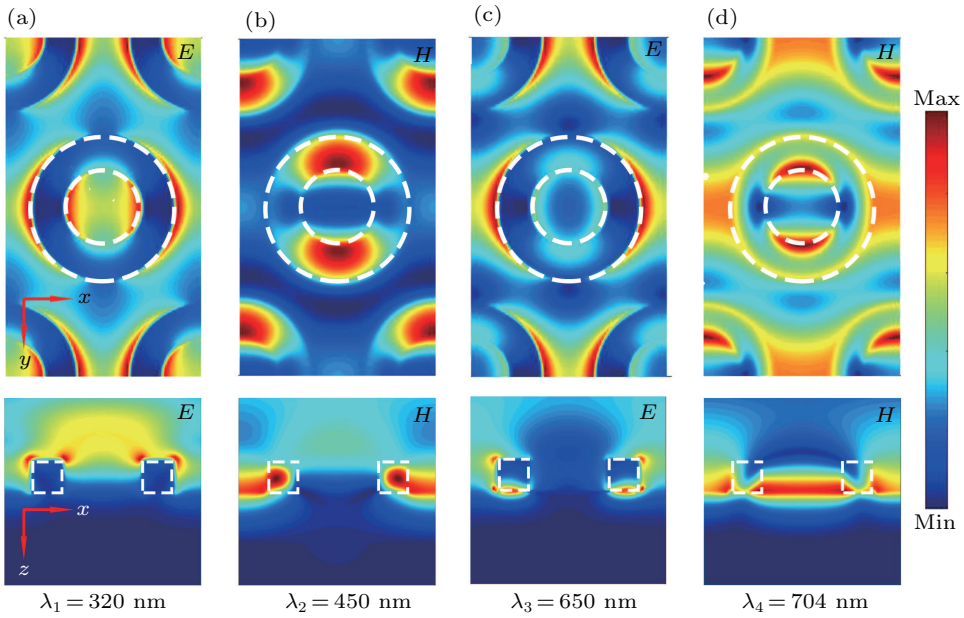


Fig. 3. (a) and (c) Normalized electric intensity distributions in (a) *xoy* plane and (b) *xoz* plane for the absorption bands at λ_1 and λ_3, respectively. (b) and (d) Normalized magnetic intensity distributions in (a) *xoy* plane and (b) *xoz* plane for the absorption bands at λ_2 and λ_4, respectively.

3.2. Effect of material and geometry on absorption performance

In the design of the absorber, we make a comparison of absorption performance between the ring and disc shaped plasmonic structure design of the square and hexagonal lattice arrangement. As shown in Fig. 4(a), the hexagonal lattice arrangement is better than the square lattice arrangement, and the ring structure is superior to the disc structure in the sense of the intensity varying with wavelength. This is because the electric fields between each unit cell and its adjacent cells in the hexagonal structure interact more strongly than in the square lattice structure, resulting in stronger resonance absorption. The comparison between the disc and the ring shows that the electric field is localized mainly on the outer surface of the disc near the wavelength of 650 nm, whereas in the case of the ring structure, the electric field can be localized on both the outer and inner surfaces, due to the existence of outer surface and the inner surface. The overlapping interaction between the outer surface and the inner surface produces a stronger resonance absorption. Therefore, the circular structure of the hexagonal lattice can exhibit higher absorption efficiency than other structures, and producing a better absorption effect. Figure 4(b) shows the effect of the material of different top resonators on the absorption performance. Comparing with different semiconductor materials, the absorption effects are different due to the difference of dielectric constant. The

GaAs has the appropriate dielectric constant compared with Si as well as Ge, and the absorption effect of GaAs is the most excellent.

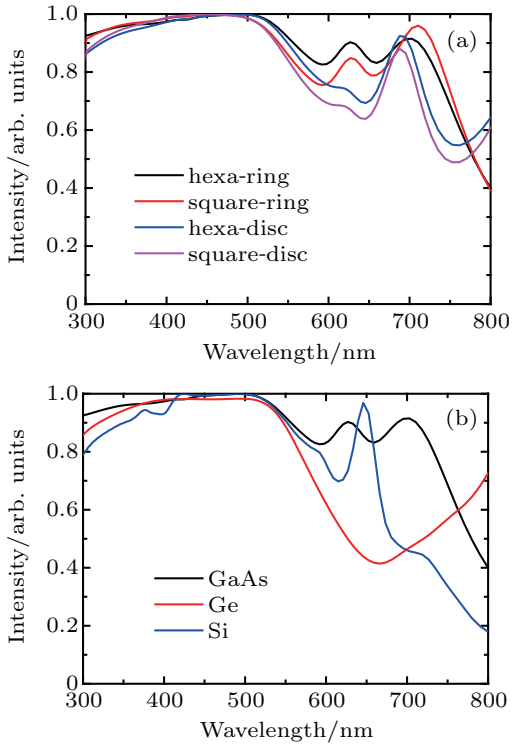


Fig. 4. (a) Comparison of absorption between hexagonal and square lattice-based disc and ring structure, (b) absorption spectra of different semiconductor materials and replacement with GaAs, Ge, and Si, respectively.

Next, we analyze the effect of the size of GaAs nanoring on absorption performance for further study. First of all, as shown in Figs. 5(a) and 5(b), we change the inner diameter d and outer diameter D of the nanoring respectively while keeping the other parameters constant. When the inner diameter d of the nanoring increases or the outer diameter D decreases, the absorption band is blue-shifted, while the absorption effect is slightly enhanced but the bandwidth is reduced. It demonstrates that as the width of the nanoring decreases, the field coupling effect in the structure increases, the width of resonance spectrum decreases, and leads the absorption band to be blue-shifted. Figure 5(c) shows the absorption evolution of the GaAs absorber under different values of thickness h of the nanoring. As the thickness is increased, the absorption spectrum shows a trend of overall red-shift, and the absorption bandwidth of the GaAs absorber is broadened, although the overall absorption effect is better only when h is 60 nm. Figure 5(d) shows the absorption evolution of the GaAs absorber under different values of period P of the nanoring. It can be seen from the figure that the absorption bandwidth remains basically the same in a minor range of periodic changes while the absorption effect is influenced by the period. As the period decreases, the absorption effect in the 500 nm–700 nm band is enhanced. That is because the gap between the adjacent nanorings becomes smaller with the period decreasing, resulting in a stronger field coupling between them, and thus the absorption effect is enhanced. However, the absorption near the wavelength of 450 nm changes very little under different geometries, because it is more related to the intrinsic properties of GaAs.

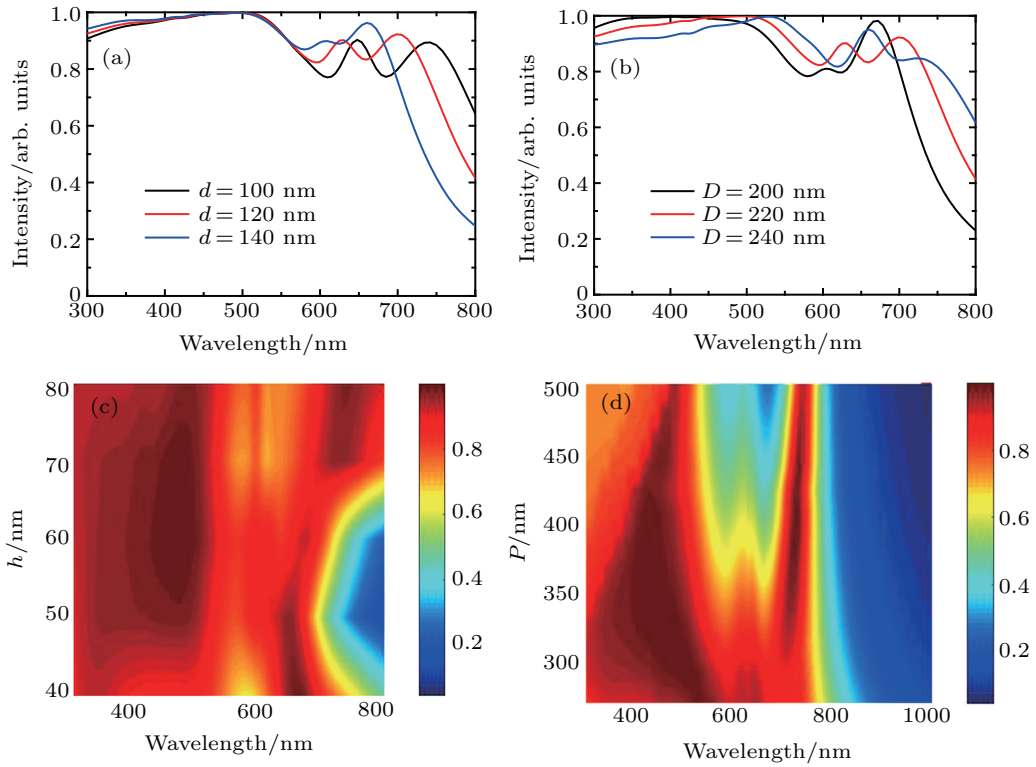


Fig. 5. Spectral curves of absorption for the GaAs absorber with (a) different inner diameter (d) values from 100 nm to 140 nm and (b) different outer diameter (D) values from 220 nm to 240 nm. Absorption mapping for GaAs absorber with (c) different thickness (h) values from 40 nm to 80 nm and (d) different period (P) values from 260 nm to 500 nm.

In addition, the absorption presents an interesting phenomenon after the period has become greater than the working wavelength. When the period is $P = 300$ nm, the absorption wavelength can extend the entire visible light region with an average absorption rate more than 90%. Increasing the period to 400 nm, the absorption rate decreases in the short wavelength range and has peak intensity at the wavelength of 400 nm. As the period increases to 500 nm, the absorption intensity further decreases, but the absorption peak appears at the wavelength of 500 nm. When the period is larger than the working wavelength, the absorption intensity decreases as the period increases. This optical property is due to the presence of higher order diffraction in the absorber.[38] These results indicate that adjusting the geometric parameters of the GaAs nanoring structures can be used to improve its absorption performance.

Then, for the ideal absorber, it is desirable to have polarization-insensitive properties. By simulating the absorption rates at different polarization angles with the proposed GaAs absorber as shown in Fig. 6, it can be observed that the absorption performance remains unchanged as the polarization angle increases, indicating that the change of the polarization angle of the incident light has little influence on the proposed broadband visible light absorber. The good polarization insensitivity of the absorber is attributed to the high symmetry of its structure. These features enable the absorber to have wide applications in optoelectronics, especially in the field of solar energy.

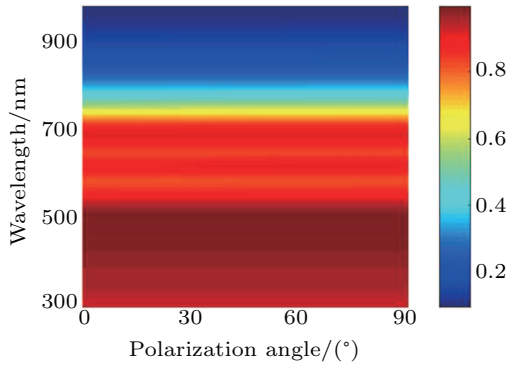


Fig. 6. Absorption mapping for GaAs absorber with different polarization angles from 0° to 90°.

4. Conclusions and perspectives

In this work, we proposed a broadband visible light absorber, which consists of a periodic hexagonal GaAs nanoring array and a gold substrate. With the absorption covering almost the entire visible light wavelength region, the GaAs absorber shows the excellent absorption performance and the average absorption rate of over 90%. Moreover, perfect absorption is achieved in a waveband of 450 nm–500 nm. The strong electrical and magnetic resonance response and the effects of the field coupling make this broadband absorption possible. In addition, the polarization insensitivity performance is particularly good, and the change in the polarization angle does not substantially affect the absorption rate. The GaAs absorber also has the advantages of simple structure, wide bandwidth, and high absorption rate. Such a broadband visible light absorber will hold potential applications in solar energy, thermal imaging and photodetectors.

Acknowledgment

The authors express their heartfelt thanks to Professor Sheng Lan for his guidance.

References

[1] Smith D R, Pendry J B and Wiltshire M C K 2004 *Science* **305** 788
[2] Cai W S and Shalaev V 2009 *Optical Metamaterials: Fundamentals and Applications* (New York: Springer) p. 59
[3] Dong J W, Zheng H H, Lai Y, Wang H Z and Chan C T 2011 *Phys. Rev. B* **83** 115124
[4] Andrea A and Engheta N 2008 *J. Opt. A: Pure Appl. Opt.* **10** 093002
[5] Pendry J B 2000 *Phys. Rev. Lett.* **85** 3966
[6] Lin W W, Li Z C, Cheng H, Tang C C, Li J J, Zhang S, Chen S Q and Tian J G 2018 *Adv. Mater.* **30** 1706368
[7] Khorasaninejad M, Chen W T, Robert C D, Jaewon O, Alexander Y Z, Federico C 2016 *Science* **352** 1190
[8] Liu W W, Li Z C, Li Z, Cheng H, Tang C C, Li J J, Chen S Q and Tian J G 2019 *Adv. Mater.* **31** 1901729
[9] Ra'di Y, Simovski C R and Tretyakov S A 2015 *Phys. Rev. Appl.* **3** 037001
[10] Landy N I, Sajuyigbe S, Mock J J, Smith D R and Padilla W J 2008 *Phys. Rev. Lett.* **100** 207402
[11] Aydin K, Ferry V E, Briggs R M and Atwater H A 2011 *Nat. Commun.* **2** 517
[12] Yan M, Dai J and Qiu M 2014 *J. Opt.* **16** 025002
[13] Yudistira H T, Liu S, Cui T J and Zhang H 2018 *Beilstein J. Nanotechnol.* **9** 1437
[14] Zhou W C, Li K W, Song C, Hao P, Chi M B, Yu M X and Wu Y H 2015 *Opt. Express* **23** 413
[15] Wang B X, Huang W Q and Wang L L 2017 *RSC Adv.* **7** 42956
[16] Behera S and Joseph J 2017 *J. Appl. Phys.* **122** 193104
[17] Shi J X, Zhang W C, Xu W, Zhu Q, Jiang X, Li D D, Yan C C and Zhang D H 2015 *Chin. Phys. Lett.* **32** 94204
[18] Li J, Verellen N and Dorpe P V 2017 *ACS Photon.* **4** 1893
[19] Liu S D, Wang Z X, Wang W J, Chen J D and Chen Z H 2017 *Opt. Express* **25** 22375
[20] Kruk S and Kivshar Y 2017 *ACS Photon.* **4** 2638
[21] Zhou X, Lai M Q, Zhang D, Deng F, Xiang J, Luo L, Lai D N, Wen W K, Fan H F, Dai Q F and Liu H Y 2018 *Opt. Commun.* **428** 47
[22] Lv J W, Mu H W, Liu Q, Zhang X M, Li X L, Liu C, Jiang S S, Sun T and Chu P K 2018 *Appl. Opt.* **57** 4771
[23] Gómez-Medina R, GarcíaC ámara B, Suárez-Lacalle I, González F, Moreno F, Nieto-Vesperinas M and Sáenz J J 2011 *J. Nanophoton.* **5** 053512
[24] Bezares F J, Long J P, Glembocki O J, Guo J P, Rendell R W, Kasica R, Shirey L, Owrutsky J C and Caldwell J D 2013 *Opt. Express* **21** 27587
[25] Pillai S, Catchpole K R, Trupke T and Green M A 2007 *J. Appl. Phys.* **101** 093105
[26] Liu Z Q, Fu G L, Huang Z P, Chen J, Pan P P, Yang Y X and Liu Z M 2017 *Mater. Lett.* **194** 13
[27] Kang D, Lee S M, Li Z W, Seyedi A, O'Brien J, Xiao J L and Yoon J 2014 *Adv. Opt. Mater.* **2** 373

[28] Hagglund C, Zeltzer G, Ruiz R, Wangperawong A, Roelofs K E and Bent S F 2016 *ACS Photon.* **3** 456

[29] Goldflam M D, Kadlec E A, Olson B V, Klem J F, Hawkins S D, Parameswaran S, Coon W T, Keeler G A, Fortune T E, Tauke-Pedretti A, Wendt J R, Shaner E A, Davids P S, Kim J K and Peters D W 2016 *Appl. Phys. Lett.* **109** 251103

[30] Argyropoulos C, Le K Q, Mattiucci N, D'Aguanno G and Alù A 2013 *Phys. Rev. B* **87** 205112

[31] Gong Y K, Wang Z B, Li K, Uggalla L, Huang J G, Copner N, Zhou Y, Qiao D and Zhu J Y 2017 *Opt. Lett.* **42** 4537

[32] Zhang K L, Hou Z L, Bi S and Fang H M 2017 *Chin. Phys. B* **26** 127802

[33] Liu X S, Chen J, Liu J S, Huang Z P, Yu M D, Pan P P and Liu Z Q 2017 *Appl. Phys. Express* **10** 111201

[34] Zhu W R, Xiao F J, Rukhlenko I D, Geng J P, Liang X L, Premaratne M and Jin R 2017 *Opt. Express* **25** 5781

[35] Ni H B, Wang M, Shen T Y and Zhou J 2015 *ACS Nano* **9** 1913

[36] Taflove A and Hagness S C 2016 *Finite-Difference Time-Domain Solution of Maxwell's Equations* (New York: John Wiley & Sons, Inc) p. 9

[37] Palik E D 1985 *Handbook of Optical Constants of Solids* (Boston: Academic Press) p. 189

[38] Liu W W, Li Z C, Cheng H, Chen S Q and Tian J G 2017 *Phys. Rev. Appl.* **8** 014012